Published in final edited form as:
J Magn Reson Imaging. 2013 January ; 37(1): 138–145. doi:10.1002/jmri.23786.

Differentiation of Malignant and Benign Breast Lesions Using Magnetization Transfer Imaging and Dynamic Contrast-enhanced MRI

Samantha L. Heller, MD, PhD[1], **Linda Moy, MD**[1], **Sherlin Lavianlivi, MD**[1], **Melanie Moccaldi**[1], and **Sungheon Kim, PhD**[1]

[1]Radiology, NYU School of Medicine, NY, NY, United States

Abstract

Purpose—To evaluate feasibility of using magnetization transfer ratio (MTR) in conjunction with dynamic contrast-enhanced magnetic resonance imaging (DCE-MRI) for differentiation of benign and malignant breast lesions at 3 Tesla.

Materials and Methods—This prospective study was IRB and HIPAA compliant. DCE-MRI scans followed by MT imaging were performed on 41 patients. Region of interests (ROI's) were drawn on co-registered MTR and DCE post-contrast images for breast structures, including benign lesions (BL) and malignant lesions (ML). Initial enhancement ratio (IER) and delayed enhancement ratio (DER) were calculated, as were normalized MTR, DER and IER (NMTR, NDER, NIER) values. Diagnostic accuracy analysis was performed.

Results—Mean MTR in ML was lower than in BL ($p < 0.05$); mean DER and mean IER in ML were significantly higher than in BL ($p<0.01$, $p<0.001$). NMTR, NDER, and NIER were significantly lower in ML versus BL ($p<0.007$, $p<0.001$, $p<0.001$). IER had highest diagnostic accuracy (77.6%), sensitivity (86.2%), and area under the ROC curve (.879). MTR specificity was 100%. Logistic regression modeling with NMTR and NIER yielded best results for BL versus ML (sensitivity 93.1%, specificity 80%, AUC 0.884, accuracy 83.7%).

Conclusion—Isolated quantitative DCE analysis may increase specificity of breast MR for differentiating BL and ML. DCE-MRI with NMTR may produce a robust means of evaluating breast lesions.

Keywords

breast cancer; magnetization transfer; DCE-MRI

INTRODUCTION

Screening for breast cancer with mammography has led to an approximately 30% decrease in mortality from breast cancer since 1990 (1). Nevertheless, breast cancer remains the second leading cause of cancer death in women and the primary cause of death in women aged 45 to 55 (2, 3). Mammography has well-recognized limitations, such as exposure to ionizing radiation (4) and a continued large incidence of false positives, including low sensitivity in patients with dense breasts (5). MRI has emerged as an alternative, powerful tool for breast cancer screening as it does not require exposure to ionizing radiation; it is

Correspondence to: Samantha L. Heller, MD New York University School of Medicine Department of Radiology 550 First Avenue New York, NY 10016 Samantha.Heller@nyumc.org Tel: 917 951-4760 .

thus safe to use routinely and more suitable than mammography for assessing young women. MRI, particularly dynamic contrast enhanced MRI (DCE-MRI), has been used for breast tumor assessment with promising results (6, 7). But multiple studies have noted that the specificity of DCE-MRI is highly variable (6-10). Pharmacokinetic model analysis of DCE-MRI data has been shown to improve diagnostic accuracy in assessing breast cancer, but frequently requires acquisition of high temporal resolution images and sophisticated, time-consuming analysis, neither of which may be readily available for routine clinical exams (9, 11). In this study, we hypothesized that the diagnostic accuracy of DCE-MRI can be improved in combination with magnetization transfer imaging (MTI).

MTI exploits the interactions of water protons with different macromolecular environments. In the simplest of models, protons in tissue are considered to reside in distinct environments: a “free” water proton pool yielding the conventionally visible MRI signal and a “restricted” proton pool in which the protons are bound to proteins and macromolecules. Exchange and cross-relaxation of magnetization between these two pools give rise to the MT effect (12). Such MT effect can be seen as attenuated on-resonance signal intensity when the bound protons are saturated with off-resonance radio-frequency pulses. MT ratio (MTR) is calculated from signal intensities with and without application of the off-resonance saturation pulse (13).

MTI technique has been used to study various pathologies associated with changes in macromolecular contents, such as demyelination in white matter (14). For breast MRI, Santyr et al. (15) reported in 1996 that signal intensity of fibroglandular breast tissue can be suppressed by MT which is helpful for visualizing lesions and silicone implants. While an in vitro NMR study by Callicott et al. (16) showed that quantitative MT model parameters did not provide a means of discriminating between benign and malignant tissues, recently, it was reported by Bonini et al. (17) that the MTR of malignant breast cancer lesions in vivo was significantly lower than that of benign lesions at 1.5T. However, it has not been shown whether MTI alone or combined with DCE-MRI can provide a better diagnostic accuracy than DCE-MRI alone.

The purpose of this study was therefore to evaluate the feasibility of using MTR in conjunction with DCE-MRI for differentiation of benign and malignant lesions. In addition, this study was performed at 3T in order to assess whether the significant difference between the malignant and benign lesions found by Bonini et al. (17) can also be observed at a higher field strength of 3T.

MATERIALS AND METHODS

Patient Data

This study was reviewed by the Institutional Review Board and was in compliance with Health Insurance Portability and Accountability Act. Written informed consent was obtained from all subjects before the scans. Data were acquired from patients (n = 41) who presented for diagnostic MRI scans. The patients ranged in age from 39 to 70 years, with a mean age of 50.9 years. The majority of patients (36/41) (88%) presented with a history of recently diagnosed breast cancer and were being evaluated for extent of disease.

The presence of benign lesions (BL) and malignant lesions (ML) was determined by correlating initial MR scan imaging with targeted fine needle aspiration, MR or ultrasound-guided core biopsy results, and/or lumpectomy or mastectomy results. In total, 29 ML and 21 BL were identified on the MR exams with pathology determined by ultrasound or MR-guided core biopsy and/or needle localization and lumpectomy. Final surgical excision pathology for malignant lesions identified on MR core biopsy was also reviewed when

available. All cases of BL proved to be fibrocystic change on pathology. ML included pathology proven invasive ductal carcinoma (n=9), ductal carcinoma in situ (n=8) and mixed pathology (invasive ductal carcinoma and ductal carcinoma in situ, n=11). There was also one case of pleomorphic LCIS with calcifications noted on histology. (See Table 1.)

Data Acquisition

A whole body Siemens 3T Tim Trio system (Siemens, Erlangen, Germany) and a 7-element breast coil (In Vivo, Orlando, FL) were employed for the scans. DCE-MRI scan was performed as a part of standard diagnostic breast exam protocol at our institution which also includes T1 weighted images with and without fat suppression and post-contrast T2 weighted images. DCE-MRI data was acquired using a 3D volume interpolated breathhold exam (VIBE) sequence (18) with Repetition Time (TR) = 4.01 ms, Echo Time (TE) = 1.52 ms, resolution 1.4 × 0.9 × 1.5 mm for five consecutive frames (90 s / frame). A single dose of Gd-DTPA (Magnevist, Bayer, Germany) with concentration of 0.1 mmol/kg body weight was injected at 2 ml/sec into an antecubital vein, followed by saline flush with a power injector (Medrad, Indiana, PA) after the first frame. Following routine diagnostic scans including DCE-MRI (approximately 15 min after contrast injection), MTI was conducted using a 3D fast low angle shot (FLASH) sequence with TR = 32 ms, TE = 2.37 ms, Flip Angle (FA) = 10°, Integrated Parallel Acquisition Techniques (iPAT) = 2 and spatial resolution = 1.2 × 1.2 × 2 mm covering the entire breast. This sequence was run three times; first one without a MT saturation pulse, second one with a MT saturation pulse (500° effective pulse angle at 1.2 kHz off-resonance for 10 ms), and third one without a MT saturation pulse, for a total of 5 min. In this study, we used the default option of MT contrast provided in the gradient echo sequence from the scanner manufacturer. The shape of the pulse was Gaussian and the effective bandwidth was 187 Hz. The average of the first and third scans was used as the MT-off image, in order to minimize the effect of the slow washout of the contrast agent which could have otherwise caused variation of tissue T1. The total scan time for both MTI and DCE-imaging was approximately 12 min. The total scan time for conventional imaging and research protocols combined was 27 minutes.

Image Analysis

Prior to data analysis, DCE MR images were co-registered to MT images using a 3D registration with affine transformation and mutual information using Statistical Parametric Mapping (SPM) (University College London, United Kingdom), an image processing software. Quality of the registration was visually assessed by one radiologist and was found to be acceptable as both MTI and DCE scans were done within the same session, and there was no substantial change of breast position in between. MTR was calculated as the difference between MT-on and MT-off, divided by MT-off. Normalized MTR (NMTR) was calculated by dividing the MTR of ML or BL by the MTR of the pectoralis muscles. Percentage increase of the signal between the first (pre-contrast) and second (first post-contrast) DCE-MRI series was calculated and referred to as Initial Enhancement Ratio (IER). Percent increase of the signal between the first (precontrast) and the fifth (last post-contrast) series was calculated and referred to as the delayed enhancement ratio (DER). Normalized IER and DER (NDER, NIER) were also calculated to account for interpatient variability in cardiovascular function and/or contrast injection timing by dividing by the averaged signal of the right and left internal mammary arteries (IMA), one of the major arteries of the breast. Regions of interest (ROI) were drawn on the co-registered post-contrast images by a breast radiologist (one year of specialty training) (S.H.) for the following structures: adipose tissue (AT), pectoralis muscle (PM), fibroglandular tissue (FG), bilateral internal mammary arteries (IMA), pathology proven BL and pathology proven ML. One ROI was drawn per lesion. In addition to the quantitative parameters such

as IER and DER, conventional kinetic curve analysis (Type 1, 2, and 3) of each lesion was performed.

Statistical Analysis

Mean MTR, DER, and IER values of the various tissue types were compared using a two-tailed t-test with unequal variance. Also, the diagnostic accuracy of MTR, DER, and IER was evaluated in terms of sensitivity, specificity and an area under receiver operating characteristic (ROC) curve (AUC). A cutoff value for each parameter was determined by maximizing the sum of sensitivity and specificity, also known as the Youden index (19, 20). A univariate logistic regression analysis was used to evaluate the predictive power of individual parameters. A multivariate logistic regression analysis was also performed to determine an optimal logistic regression model for differentiation of two legion types. A leave-one-out cross-validation was used for all analysis. Data analysis was conducted by using the Statistical Package for the Social Sciences for Windows, Version 17.0 (SPSS Inc, Chicago, IL).

RESULTS

Figure 1 shows representative images of post-contrast image, MTR, IER, and DER from a patient with invasive ductal carcinoma. Note that MTR signal of the lesion is lower in signal intensity than the surrounding stroma while IER signal intensity is markedly higher than the surrounding stroma.

Conventional kinetic curve analysis on the lesions was performed using a computer-aided diagnosis system (DynaCAD; Invivo) to acquire conventional kinetic curve information (Type 1, Type 2 or Type 3 curves) for each lesion (Table 2). The majority of lesions with a Type 3 kinetic curve were malignant; however, eight of the malignant lesions (28%) demonstrated a Type 1 kinetic curve of which two were invasive cancers. One benign lesion (5%) demonstrated a Type 3 kinetic curve. Seven malignant lesions (24%) and nine benign lesions (43%) had indeterminate or Type 2 kinetic curves.

Figure 2 shows comparison of MTR and DCE data across different breast tissue types. The mean MTR of malignant lesions was significantly lower ($p = 0.027$) than that of benign lesions. The mean DER of ML was significantly higher than that of BL ($p < 0.01$) and the mean IER of ML was also significantly higher than that of BL ($P < 0.001$). The diagnostic accuracy measures of MTR, DER, and IER are summarized in Table 3. Diagnostic accuracy of MTR alone was low (51%). IER had the highest diagnostic accuracy (77.6 %), AUC (. 879) and sensitivity (86.2 %). The best logistic regression model was to use IER alone. The combination of MTR and IER did not lead to significant improvement. MTR had the lowest sensitivity (40 %) and highest specificity (100 %).

Figure 3 shows MTR and DCE data normalized to those of the pectoralis and the internal mammary arteries, respectively. The mean NMTR of malignant lesions was significantly lower than that of BL ($p<0.007$). Likewise, the mean NDER and NIER of malignant lesions were significantly higher than those of benign lesions ($p<0.001$ for each data set). Of NMTR, NDER, and NIER, NIER had the highest sensitivity (93.1%), but had a low specificity (75%) (Table 4). NMTR alone had a low diagnostic accuracy (67.3%). The best logistic regression model based on the normalized parameters included NMTR and NIER, yielding a sensitivity of 93.1%, a specificity of 80% and an accuracy of 83.7%.

$$f(NMTR, NIER) = \frac{1}{1+\exp\left[-(\beta_0+\beta_1 NMTR+\beta_2 NIER)\right]}$$

where $\beta 0 = 2.43$, $\beta 1 = -8.17$, and $\beta 2 = 9.76$. The cutoff value for the model was 0.43 with sensitivity = 93.1%, specificity = 80%, AUC = 0.884 and accuracy = 83.7% based on leave-one-out cross-validation.

Figure 4 demonstrates an invasive malignant lesion with a Type 1 curve and a benign lesion with a Type 3 kinetic curve. Regression NMTR+NIER output value for the malignant lesion (Figure 4a) was 0.75, above the cut-off of 0.43, a value consistent with malignancy. Regression NMTR+NIER output value for the benign lesion (Figure 4b) was 0.01, below the cut-off of 0.43, a value consistent with benignity.

DISCUSSION

Contrast-enhanced MRI is a powerful imaging tool that has shown utility in delineating extent of disease in patients with known breast cancer and in screening women at high risk for breast cancer. It has been shown to have very high sensitivity for detecting malignancy, with a broad range of specificity (21, 22). Quantitative analysis of DCE-MRI data is one means of increasing the specificity of the breast MR examination (23). DCE-MRI relies upon the relaxivity of contrast agents in T1-weighted imaging. Signal enhancement as a property of the rate of T1 relaxation is theoretically proportional to contrast agent concentration and can be measured over time (24). DCE-MRI exploits the increased and abnormal vascularity that may occur with breast malignancies, allowing comparison of contrast uptake over time in lesions versus in normal fibroglandular breast tissue (25).

Clinical use of lesion kinetics most frequently relies on a qualitative assessment of kinetic curve parameters (initial enhancement is defined as slow, medium, or rapid and shape of the time signal intensity curve is defined as Type I persistent, Type 2 plateau and Type 3 wash-in/wash-out curves) indicating likelihood of benignity or malignancy (26). Although as shown in Kuhl and colleagues' seminal 1999 study of signal intensity time course data, the majority of benign lesions have a Type 1 curve, and the majority of malignant lesions have a Type 3 curve, there is overlap within these categories (26, 27). Multiple studies have also shown such qualitative analyses to be variable (28, 29) with AUC reported at .66 to .77 (23, 30). This overlap is also seen in our own qualitative kinetic evaluation results as demonstrated in Table 2.

However, more recent work has begun focusing on means of quantitatively analyzing available kinetic information with the aim of increasing specificity in distinguishing benign from malignant lesions. This may be performed in a variety of ways. For example many studies employ what Bonekamp and colleagues, in their review of prostate DCE, describe as an heuristic approach based on assumptions regarding contrast concentration (31). Such methods include determining the slope of the first pass and the time to peak or calculating slope of the washout curve (23, 31). As Bonekamp and colleagues point out, this approach has been found to correlate with cancer detection in multiple studies, but findings may vary considerably based on underlying factors such as hardware and contrast dose.

Another approach is to invoke pharmacologic models which attempt to explain the mechanics of enhancement in light of physiologic distribution of contrast from the intravascular to the extravascular space (27). There are multiple pharmacological models invoking differing numbers of compartments, equations for input, output, and flux/gradient of tracer across compartments, and parameters such as blood flow, endothelial permeability, and vascular surface area (24, 31). A commonly used estimate of inflow, for example, is the vascular transfer constant (K^{trans}), a function of blood flow and vascular permeability.

At present, pharmacologic models are often based upon a variety of different assumptions which result in difficulty in comparing results. As an example, while standard models of

DCE-MRI assume that equilibrium transcytoluminal water exchange is infinitely fast, newer work on breast cancer (28, 32) and head and neck cancer (33) has shown that this may underestimate K^{trans} for malignant lesions. Therefore, while these pharmacologic models are a promising means of distinguishing between benign and malignant lesions, at present, there are many challenges to incorporating their use, including lack of standardization of techniques and variety in modeling assumptions as well as the difficulty of acquiring DCE-MRI data with sufficiently high temporal and high spatial resolution for diagnostic purposes (24). In contrast, our approach of relatively simple calculation may be performed without extensive post-processing on typical dynamic images acquired during clinical breast MR exams.

The results of this study for MTR are consistent with those reported by Bonini et al. (17) and suggest that MTR, as well as DER and IER, may be useful parameters for differentiating between benign and malignant tissues, especially given the poor specificity of a conventional kinetic curve analysis. Our MTR data showed a significant difference between the means of BL versus ML, presumably due to differences in the macromolecular contents of tumor versus benign tissue. At present, it is not completely understood why MTR affects malignant lesions differently than benign lesions in the breast. One clue may lie in the changes in collagen in malignant lesions. Falzon and colleagues (34) investigated how breast cancer results in major changes in the structure of the collagenous component of the extra-cellular matrix. After analysis of normal tissue, benign breast lesion tissue, and malignant breast lesion tissue, they determined that there were “major differences” in the shape of collagen fibers in malignant disease; these alterations could explain the alteration in MT signal noted in our study since MT F

We assumed that DCE measures in the IMA can be used to correct for systemic changes that might affect DCE measures in the breast tissue. Normalizing DCE measures to the internal mammary arteries resulted in improved diagnostic accuracy, likely by compensating any variability in injection timing and/or cardiac function. Normalizing MTR of the lesions to that of the pectoralis muscle also improved its diagnostic accuracy as it likely compensated for any systemic variation, including B0 and B1 inhomogeneities between subjects. However, we found that MTR alone does not provide a high enough accuracy, but the best results were obtained by a logistical regression model of normalized IER and MTR. This result implies that MTR provides complementary information which in conjunction with NIER data yields greater diagnostic accuracy in distinguishing between malignant and benign lesions.

Limitations of our study include our relatively small sample size and the fact that ROI’s were drawn without blinding the reader to the final pathologic diagnosis of the lesion which may have caused bias in regard to drawing lesion boundaries. In addition, in our study, MT imaging was performed after clinical routine scans which included contrast injection. In order to minimize the effect of T1 change during the slow washout phase, we acquired MT-off scans before and after MT-on sequence and used the average of MT-off scans to calculate MTR. Although the MT effect could be reduced by contrast agents (13), we were able to see a significant difference in MTR between benign and malignant lesions. Future study is warranted to investigate if pre-contrast MTR can differentiate malignant and benign lesions better than post-contrast MTR used in this study.

In conclusion, our results suggest that quantitative DCE analysis may increase specificity of breast MR for differentiating malignant lesions from benign ones and MTR analysis may be of potential use as the mask image in clinical MRI breast studies, decreasing the confounding factor of physiologic enhancement. In addition, employing DCE in conjunction with MTR may produce a robust means of evaluating breast lesions. Further evaluation of

MTR and DCE-MRI with a greater number of cases is required to determine if these techniques can increase the specificity of breast MRI.

Acknowledgments

Grant Support: National Institutes of Health 1UL 1RR029893-01

REFERENCES

1. Lee CH, Dershaw DD, Kopans D, et al. Breast cancer screening with imaging: recommendations from the Society of Breast Imaging and the ACR on the use of mammography, breast MRI, breast ultrasound, and other technologies for the detection of clinically occult breast cancer. J Am Coll Radiol. 2010; 7:18–27. [PubMed: 20129267]
2. Society, AC. Breast Cancer Facts & Figures 2009-2010. American Cancer Society, Inc; Atlanta: 2009.
3. Jemal A, Siegel R, Ward E, Hao Y, Xu J, Thun MJ. Cancer statistics, 2009. CA Cancer J Clin. 2009; 59:225–249. [PubMed: 19474385]
4. Samei E, Saunders RSJ, Baker JA, Delong DM. Digital mammography: effects of reduced radiation dose on diagnostic performance. Radiology. 2007; 243:396–404. [PubMed: 17356178]
5. Fenton JJ, Taplin SH, Carney PA, et al. Influence of computer-aided detection on performance of screening mammography. N Engl J Med. 2007; 356:1399–1409. [PubMed: 17409321]
6. Saslow D, Boetes C, Burke W, et al. American Cancer Society guidelines for breast screening with MRI as an adjunct to mammography. CA Cancer J Clin. 2007; 57:75–89. [PubMed: 17392385]
7. Lehman CD, Gatsonis C, Kuhl CK, et al. MRI evaluation of the contralateral breast in women with recently diagnosed breast cancer. N Engl J Med. 2007; 356:1295–1303. [PubMed: 17392300]
8. Williams TC, DeMartini WB, Partridge SC, Peacock S, Lehman CD. Breast MR imaging: computer-aided evaluation program for discriminating benign from malignant lesions. Radiology. 2007; 244:94–103. [PubMed: 17507720]
9. Huang W, Li X, Morris EA, et al. The magnetic resonance shutter speed discriminates vascular properties of malignant and benign breast tumors in vivo. Proc Natl Acad Sci U S A. 2008; 105:17943–17948. [PubMed: 19004780]
10. Kriege M, Brekelmans CT, Boetes C, et al. Efficacy of MRI and mammography for breast-cancer screening in women with a familial or genetic predisposition. N Engl J Med. 2004; 351:427–437. [PubMed: 15282350]
11. Li X, Huang W, Yankeelov TE, Tudorica A, Rooney WD, Springer CSJ. Shutter-speed analysis of contrast reagent bolus-tracking data: Preliminary observations in benign and malignant breast disease. Magn Reson Med. 2005; 53:724–729. [PubMed: 15723402]
12. Wolff SD, Balaban RS. Magnetization transfer contrast (MTC) and tissue water proton relaxation in vivo. Magn Reson Med. 1989; 10:135–144. [PubMed: 2547135]
13. Henkelman RM, Stanisz GJ, Graham SJ. Magnetization transfer in MRI: a review. NMR Biomed. 2001; 14:57–64. [PubMed: 11320533]
14. Grossman RI, Gomori JM, Ramer KN, Lexa FJ, Schnall MD. Magnetization transfer: theory and clinical applications in neuroradiology. Radiographics. 1994; 14:279–290. [PubMed: 8190954]
15. Santyr GE, Kelcz F, Schneider E. Pulsed magnetization transfer contrast for MR imaging with application to breast. J Magn Reson Imaging. 1996; 6:203–212. [PubMed: 8851429]
16. Callicott C, Thomas JM, Goode AW. The magnetization transfer characteristics of human breast tissues: an in vitro NMR study. Phys Med Biol. 1999; 44:1147–1154. [PubMed: 10368008]
17. Bonini RH, Zeotti D, Saraiva LA, et al. Magnetization transfer ratio as a predictor of malignancy in breast lesions: preliminary results. Magn Reson Med. 2008; 59:1030–1034. [PubMed: 18429009]
18. Rofsky NM, Lee VS, Laub G, et al. Abdominal MR imaging with a volumetric interpolated breath-hold examination. Radiology. 1999; 212:876–884. [PubMed: 10478260]
19. Zou KH, O'Malley AJ, Mauri L. Receiver-operating characteristic analysis for evaluating diagnostic tests and predictive models. Circulation. 2007; 115:654–657. [PubMed: 17283280]

20. Perkins NJ, Schisterman EF. The Youden Index and the optimal cut-point corrected for measurement error. Biom J. 2005; 47:428–441. [PubMed: 16161802]
21. Bone B, Aspelin P, Bronge L, Isberg B, Perbeck L, Veress B. Sensitivity and specificity of MR mammography with histopathological correlation in 250 breasts. Acta Radiol. 1996; 37:208–213. [PubMed: 8600964]
22. Stomper PC, Herman S, Klippenstein DL, et al. Suspect breast lesions: findings at dynamic gadolinium-enhanced MR imaging correlated with mammographic and pathologic features. Radiology. 1995; 197:387–395. [PubMed: 7480682]
23. El Khouli RH, Macura KJ, Jacobs MA, et al. Dynamic contrast-enhanced MRI of the breast: quantitative method for kinetic curve type assessment. AJR Am J Roentgenol. 2009; 193:W295–300. [PubMed: 19770298]
24. Paldino MJ, Barboriak DP. Fundamentals of quantitative dynamic contrast-enhanced MR imaging. Magn Reson Imaging Clin N Am. 2009; 17:277–289. [PubMed: 19406359]
25. Kuhl CK, Schild HH. Dynamic image interpretation of MRI of the breast. J Magn Reson Imaging. 2000; 12:965–974. [PubMed: 11105038]
26. Kuhl CK, Mielcareck P, Klaschik S, et al. Dynamic breast MR imaging: are signal intensity time course data useful for differential diagnosis of enhancing lesions? Radiology. 1999; 211:101–110. [PubMed: 10189459]
27. Moon M, Cornfeld D, Weinreb J. Dynamic contrast-enhanced breast MR imaging. Magn Reson Imaging Clin N Am. 2009; 17:351–362. [PubMed: 19406363]
28. Kinkel K, Helbich TH, Esserman LJ, et al. Dynamic high-spatial-resolution MR imaging of suspicious breast lesions: diagnostic criteria and interobserver variability. AJR Am J Roentgenol. 2000; 175:35–43. [PubMed: 10882243]
29. Stoutjesdijk MJ, Futterer JJ, Boetes C, van Die LE, Jager G, Barentsz JO. Variability in the description of morphologic and contrast enhancement characteristics of breast lesions on magnetic resonance imaging. Invest Radiol. 2005; 40:355–362. [PubMed: 15905722]
30. Schnall M, Orel S. Breast MR imaging in the diagnostic setting. Magn Reson Imaging Clin N Am. 2006; 14:329–37. vi. [PubMed: 17098174]
31. Bonekamp D, Jacobs MA, El-Khouli R, Stoianovici D, Macura KJ. Advancements in MR imaging of the prostate: from diagnosis to interventions. Radiographics. 2011; 31:677–703. [PubMed: 21571651]
32. Huang W, Tudorica LA, Li X, et al. Discrimination of Benign and Malignant Breast Lesions by Using Shutter-Speed Dynamic Contrast-enhanced MR Imaging. Radiology. 2011
33. Kim S, Quon H, Loevner LA, et al. Transcytolemmal water exchange in pharmacokinetic analysis of dynamic contrast-enhanced MRI data in squamous cell carcinoma of the head and neck. J Magn Reson Imaging. 2007; 26:1607–1617. [PubMed: 17968962]
34. Falzon G, Pearson S, Murison R. Analysis of collagen fibre shape changes in breast cancer. Phys Med Biol. 2008; 53:6641–6652. [PubMed: 18997272]

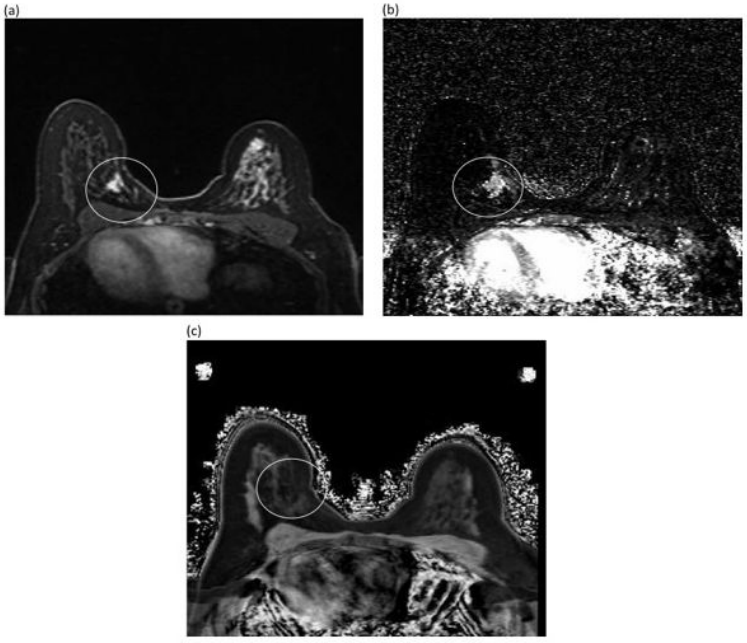

Figure 1.
Representative images acquired from a woman with known metastatic left breast cancer: (a) post-gadolinium image (b) MTR image (c) IER image. The MTR signal of the lesion (1b, white circle) is qualitatively lower in signal intensity than the surrounding fibroglandular tissue while the IER signal intensity of the lesion (1c, white circle) is qualitatively higher than the surrounding stroma.

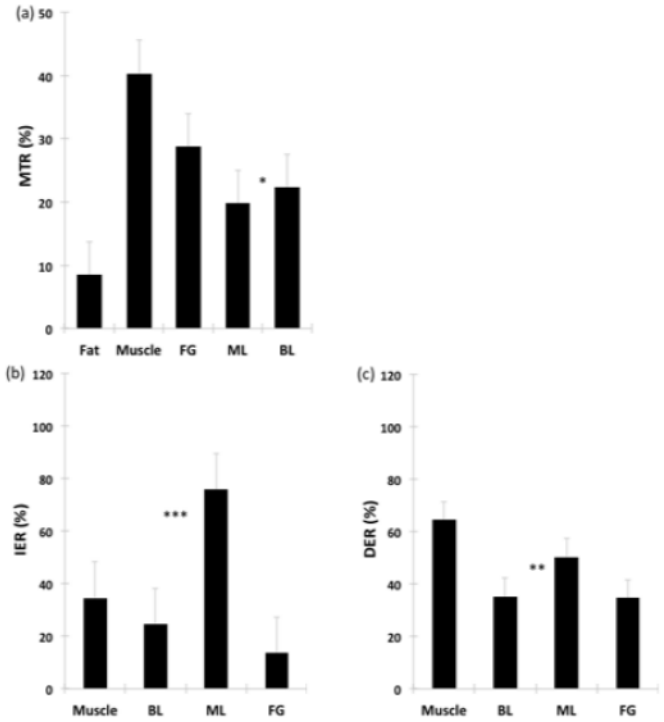

Figure 2.

Comparison of Mean MTR (a), IER (b), and DER (c) Values for Breast Tissues and Lesions. * indicates significant difference with $p < 0.05$ from two-tailed t-test with unequal variance, ** for $p < 0.01$, and *** for $p < 0.001$. Abbreviations: MTR=magnetization transfer ratio, IER = initial enhancement ratio; DER=delayed enhancement ratio; FG=fibroglandular tissue, ML=malignant lesions, BL=benign lesions.

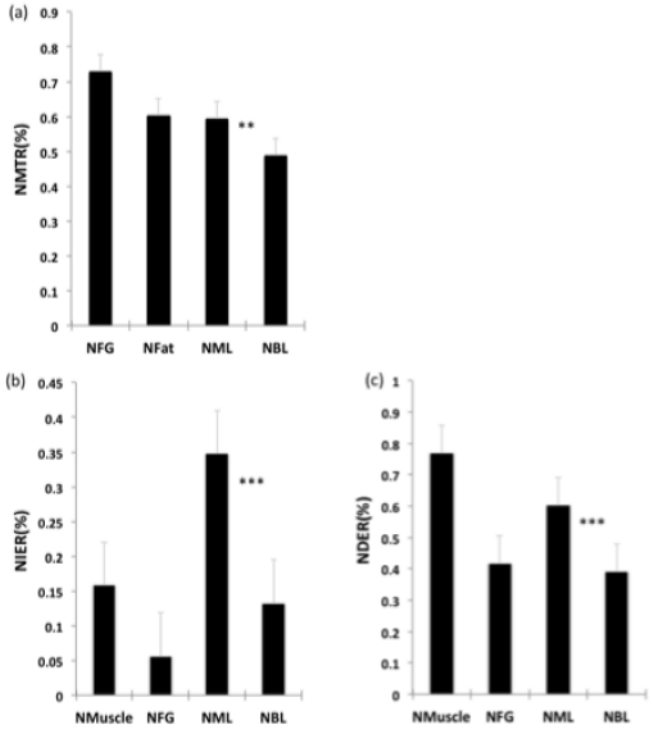

Figure 3.

Comparison of mean NMTR (a), NIER (b), and NDER (c) values for breast tissues and lesions. * indicates significant difference with $p < 0.05$ from two-tailed t-test with unequal variance, ** for;$p < 0.01$, and *** for $p < 0.001$.

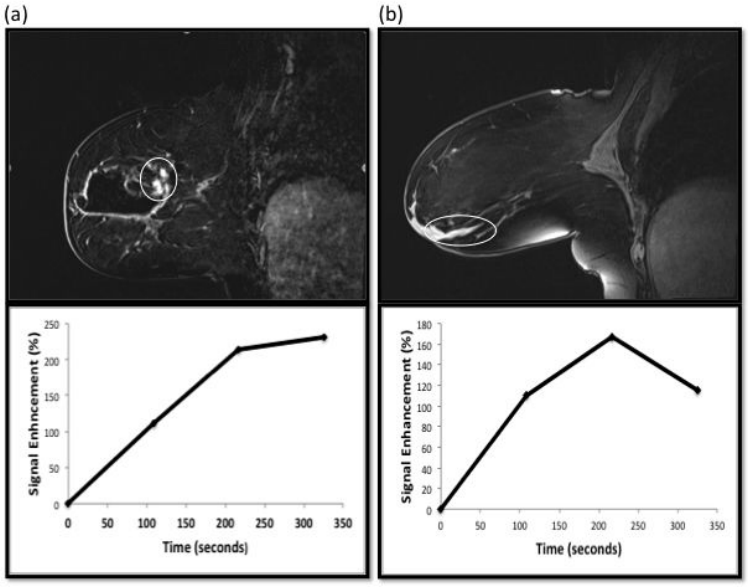

Figure 4.

(a) Post-Gd image and dynamic enhancement curve of a ML case with Type 1 curve. The patient had a recent excisional biopsy yielding DCIS. Clumped non-mass-like enhancement (NMLE) at the surgical cavity superior, posterior, and medial margins demonstrated Type 1 kinetic curves (white circle). However, DCIS and IDC were identified on re-excision. Regression NMTR+NIER output value for this lesion was 0.75, above the cut-off of 0.43, a value consistent with malignancy. (2b) Post-Gd image and dynamic enhancement curve images from a patient with a history of recently biopsied DCIS. A region of curvilinear ductal enhancement demonstrating a Type 3 kinetic curve was identified on the MR study and thought to represent malignancy (white circle). However, no malignancy was identified after lumpectomy. Regression NMTR+NIER output value for this lesion was 0.01, below the cut-off of 0.43, a value consistent with benignity.

Table 1

Size Range and Stage or Grade for Malignant Lesions

Lesion Pathology	Size range	Stage if IDC or Grade if DCIS alone (number of cases)
IDC	0.7-6 cm	Stage I (13) Stage IIA (3) Stage IIB (2) Stage IIIA (1) NA (1) *
DCIS	0.4-3 cm	Grade 1 (0) Grade 2 (3) Grade 3 (5)
LCIS	11 cm	NA (1)

* Stage not available for one lesion that was diagnosed on core biopsy without subsequent surgical excision. Abbreviations: IDC, invasive ductal carcinoma; DCIS, ductal carcinoma in situ; LCIS, lobular carcinoma in situ; NA, not applicable.

Table 2

Conventional Kinetic Curve Types for all Malignant and Benign Lesions

Kinetic Curve	ML	BL
Type 1	8/29 (27%)	11/21 (52%)
Type 2	7/29 (24%)	9/21 (43%)
Type 3	14/29 (48%)	1/21 (5%)

Abbreviations: ML=malignant lesions, BL=benign lesions

Table 3

Diagnostic accuracy of MTR and DCE data

	Cut-off	Sensitivity (95% CI)	Specificity (95% CI)	AUC (95% CI)	Accuracy (%)	Cross-validation (%)
MTR	23.8	100 (85.4, 100)	40.0 (20, 63.6)	0.64 (0.48, 0.81)	51.0	49.0
IER	35.6	86.2 (67.4, 95.5)	75.0 (50.6, 90.4)	0.88 (0.78, 0.98)	77.6	77.6
DER	39.1	79.3 (59.7, 91.3)	70.0 (45.7, 87.2)	0.79 (0.65, 0.92)	65.3	65.3

Abbreviations: AUC, area-under-the-curve; CI, confidence interval; MTR, magnetization transfer ratio; IER, initial enhancement ratio; DER, delayed enhancement ratio.

Table 4

Diagnostic accuracy of normalized MTR and DCE data.

	Cut-off	Sensitivity (95% CI)	Specificity (95% CI)	AUC (95% CI)	Accuracy (%)	Cross-validation (%)
NMTR	0.56	79.3 (59.7, 91.3)	60.0 (36.4, 80.0)	0.70 (0.53, 0.86)	67.3	65.3
NIER	0.12	93.1 (75.8, 98.8)	75.0 (50.6, 90.4)	0.86 (0.75, 0.97)	71.4	71.4
NDER	0.41	89.7 (71.5, 97.3)	60.0 (36.4, 80)	0.79 (0.67, 0.92)	69.4	69.4
NMTR + NIER	0.43	93.1 (75.8, 98.8)	80.0 (55.7, 93.4)	0.88 (0.78, 0.99)	83.7	83.7

Abbreviations: AUC, area-under-the-curve; CI, confidence interval; NMTR, normalized magnetization transfer ratio; NIER, normalized initial enhancement ratio; NDER, normalized delayed enhancement ratio